An Object Color Transformation Scheme using Regression Analysis

[1,a]Pei-Chung Chung, [2,b]Kai-Wen Chuang, [3,c]Chen-Chung Liu, [4,a,d]Chun-Yuan Yu and [5,e]Cheng-Chih Huang*

Abstract

Object's colors are frequently changed for enhancing some potential features of objects for wide applications in different fields. In this paper, target and source objects are extracted from target and source images by employing color objects extraction algorithm and by using multiple thresholds (COEMT), respectively. Multiple regression analysis (MRA) is respectively conducted on the R, G, and B planes of the target and source objects to find the corresponding best fitting function of each plane. The new values of pixels of target objects are evaluated by these best fitting functions. The final target objects are yielded by combining these new values. The experimental results show that the presented approach has three major advantages: (i) the proposed algorithm is simple, effective and accurate in transferring color between objects without any change in the object details, (ii) the proposed algorithm is time saving, (iii) there are no restrictions in the dynamic ranges of colors of objects.

Keywords: Object, image, multiple regression analysis, multiple threshold.

[a]*Department of Computer Science and Engineering, National Chung-Hsing University, Taichung 400, Taiwan*
[b]*Department of Research and Design, Feiloli Electronic Limited Company, Changhua, Taiwan*
[c]*Department of Department of Electronic Engineering, National Chin-Yi University of Technology, Taiping, Taichung 411, Taiwan*
[d]*Department of Digital Living Innovation, Nai-Kai University of Technology, Tsao-Tuen, Nantou, Taiwan*
[e]*Center of General Education, National Taichung University of Science and Technology, Taichung, Taiwan*
[1]*iam.abaw@gmail.com;* [2]*kevin017224@hotmail.com;*
[3]*ccl@ncut.edu.tw;* [4]*t112@nkut.edu.tw;* [5]*jimhuang@nutc.edu.tw*

1. Introduction

Color is a significant feature of information for image classification, segmentation, recognition, analysis, and retrieval [1]. It offers artists with the ability to show style and creativity [2], and also provides doctors a way to describe tissue pathology and aesthetics in dermatology and dentistry [3]. Frequently, some of the original colors in an object might not be suitable for analysis, and the colors in an object must be properly adjusted in advance. The appearance of an object can be adjusted manually to obtain specific effects but that requires advanced manipulation techniques which consume a great deal of time. If the colors of a target object can be changed according to a suitable source object, the final target object can easily satisfy the requirement. Color transferring is one of the most popular techniques to change an image's color and preserve the image's original details at the same time [4].

Color transformation between objects could be affected by that both the target object and source object are frequently composed with a variety of colors, causing numerous shades in the transformation results [5]. A number of methods have been proposed for global color transformation between images. Reinhard et al. [6] proposed a statistical based scheme. Their idea is based on transferring the original RGB color images into the lab color space proposed by Ruderman et al. [7] in which the correlation between channels is minimized and the color perception can be evaluated better. Thus,

they assumed that the pixel values of each channel in the lab color space is a Gaussian distribution and the color transformation process shifts and scales each channel's pixel values from the target image to match the corresponding source image mean and variance. The color transferred lab image is finally converted back into the RGB color space. The transformation is operated independently in each channel to convert a potential complex in three dimensional problems into three of simplest dimensional problems. Although this technique is simple and efficient for a large range color transformation of images, it is time consuming and overflowing that will appear when the image hue is oversaturated. C. C. Liu and G. N. Hu [8] considered the histogram in each plane of a color space as a probability density function. They first transformed the target and source images into LAB color space and then computed the probability density characteristics of each plane to find the correlation functions of the target and source images. The transferred pixel values are determined by conducting the corresponding correlation function on each target image plane. The color transferred target image is finally constructed by replacing each plane with its corresponding transferred plane.

The goal of this paper is to find a simple and efficient global color transferring approach and a measurement metrics to evaluate color transferring scheme performance. Multiple regression analysis is a statistical method used to model the relationships between several independent variables and a dependent variable by fitting an equation to the observed data. Multiple regression procedures are very widely used in social and natural sciences today [9]. It is also a pretty good technique for transferring colors from a source object to a target object. The experimental results show that the proposed algorithm is effective and validated. The remainder of this paper is organized as follows: Section 2 presents the proposed algorithm. Section 3 describes the empirical results. Section 4 concludes this paper.

2. The proposed algorithm

This paper presents a way of transferring colors from a source RGB color object to a target RGB color object. Fig. 1 is the flow chart of the recolor algorithm with multiple regression analysis. First, color object extraction algorithm with multiple thresholds (COEMT) is employed to extract target and source objects from target and source images, respectively. Multiple regression analysis is then conducted on each plane (R, G, and B planes) of target and source objects to find the corresponding best fitting functions for each plane. These best fitting functions are used to determine the new values for each pixel in the target object on each plane. These new values are then combined into the RGB recolored object. Detailed descriptions of the proposed scheme are illustrated as follows.

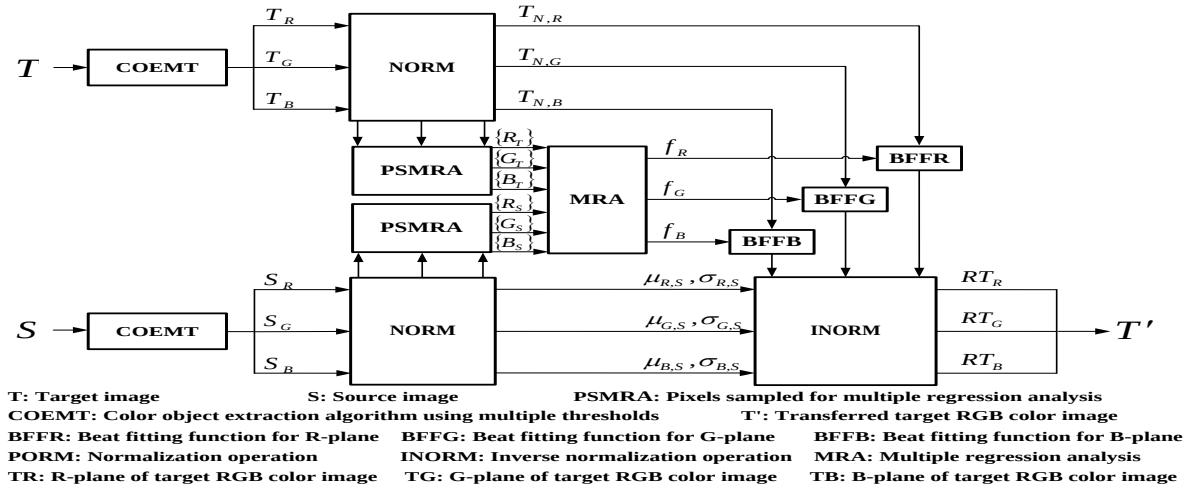

Fig. 1: The flow chart of the proposed color transformation algorithm.

2.1 Color Objects extraction algorithm using multiple thresholds (COEMT) [10]

An efficiency object extraction scheme for color images must be extreme precision and time saving. In order to construct a superior object extraction algorithm for color images, this paper combines RGB to HSI transformation, seeds distribution analysis, comparing neighbor criterion, thresholds modification, and a modified SLCCA algorithm that utilizes eight-connectivity to synthesize the color objects extraction algorithm using multiple thresholds (COEMT). The proposed COEMT is completed by the following steps: (i) at first, the users draw lines or curves at objects on the input RGB color image as markers; (ii) after the markers are drawn, the coordinates of each marker pixel are stored as the seeds for object extraction. At the same time, the input RGB color image is transformed into HSI color space; (iii) on different color planes, the adaptive forecasting filter and the corresponding threshold vectors of the first seed are generated to extract object pixels masked by the filter; (iv) the extracted object pixels are then added into the set of seeds as new seeds; (v) the extraction process is repeated according to the modified significance link and connected component analysis (MSLCCA) technique until all seeds in the seeds set are used; (vi) finally, a merge mechanism and planes union mechanism are used to get the color objects extracted from a RGB color image [10].

2.2 Multiple regression analysis (MRA)

In experiments performing, data are frequently tabulated in the form of ordered pairs $(x_1, y_1), (x_2, y_2), ..., (x_n, y_n)$ with each xi distinct. Given the data, it is then usually desirable to be able to predict y from x by finding a mathematical model, that is, a function $y = H(x)$ that fits the data as closely as possible. One way to determine how well the function $y = H(x)$ fits these order pairs $(x_1, y_1), (x_2, y_2), ..., (x_n, y_n)$ is to measure the sum of squares of the errors (SSE) between the predicted values of y and the observed values y_i for all of the n data points.

Multiple regression is one of the widely used statistical techniques [9]. This technique is used to find a polynomial function of degree k, $y = \beta_0 + \beta_1 x + \beta_2 x^2 + ... + \beta_k x^k$ as the predicting function, which has the minimum of the sum of squares of the errors(SSE) between the predicted values of y and the observed values yi for all of the n data points $(x_1, y_1), (x_2, y_2), ..., (x_n, y_n)$. The values of

$\beta_0, \beta_1, \beta_2$,…, and β_k that minimize

$$SSE(\beta_0,\beta_1,...,\beta_k)=\sum_{i=1}^{n}[y_i-(\beta_0+\beta_1 x_i+\beta_2 x_i^2+...+\beta_k x_i^k)]^2, \quad (1)$$

are obtained by setting the $k+1$ first partial derivatives $\partial(SSE(\beta_0,\beta_1,...,\beta_k))/\partial\beta_j$, $j=0,1,...,k$, equal to zero, and solves the resulting simultaneous linear system of the so-called normal equations:

$$n\beta_0+\beta_1\sum_{i=1}^{n}x_i+\beta_2\sum_{i=1}^{n}x_i^2+...+\beta_k\sum_{i=1}^{n}x_i^k=\sum_{i=1}^{n}y_i, \quad (2)$$

$$\beta_0\sum_{i=1}^{n}x_i+\beta_1\sum_{i=1}^{n}x_i^2+\beta_2\sum_{i=1}^{n}x_i^3+...+\beta_k\sum_{i=1}^{n}x_i^{k+1}=\sum_{i=1}^{n}x_i y_i, \quad (3)$$

$$\beta_0\sum_{i=1}^{n}x_i^k+\beta_1\sum_{i=1}^{n}x_i^{k+1}+\beta_2\sum_{i=1}^{n}x_i^{k+2}+...+\beta_k\sum_{i=1}^{n}x_i^{2k}=\sum_{i=1}^{n}x_i^k y_i, \quad (4)$$

and the matrix form solution of the normal equations system be

$$\begin{bmatrix}\beta_0\\ \beta_1\\ \beta_2\\ \vdots\\ \beta_k\end{bmatrix}=\mathrm{B}=\left[X^T X\right]^{-1}\left[X^T Y\right] \quad (5)$$

where

$$X=\begin{bmatrix}1 & x_1 & x_1^2 & ... & x_1^k\\ 1 & x_2 & x_2^2 & ... & x_2^k\\ 1 & x_3 & x_3^2 & ... & x_3^k\\ : & : & : & ::: & :\\ 1 & x_n & x_n^2 & ... & x_n^k\end{bmatrix}, \quad Y=\begin{bmatrix}y_1\\ y_2\\ \vdots\\ y_n\end{bmatrix}. \quad (6)$$

2.3 Best fitting functions determination

At the beginning of the process, the R, G, and B planes of the normalized target RGB color object and the normalized source RGB color object are uniformly split into *n* non-overlapping blocks respectively. The mean of each block is served as the input data for multiple regression analysis. Fig. 2 shows an example of determining the source data and target data for multiple regression analysis. In Fig. 2, (a1) shows the target RGB color image: a girl in a blue dress, (a2) shows the marks (seeds) on the original target image: four yellow points on the blue dress, (a3) the target object extracted by the proposed COEMT: the blue dress on the girl, (a4) is the corresponding histograms of the target object on each plane, (a5) is the input target data for multiple regression analysis and (a6) is the histograms of the input target data; (b1) shows the source RGB color image: wild chrysanthemum plants, (b2) shows the marks (seeds) on the original source image: a red line segment on the yellow chrysanthemum, (b3) the source object is extracted by the proposed COEMT: a yellow chrysanthemum, (b4) is the corresponding histograms of the source object on each plane, (b5) is the input source data for multiple regression analysis and (b6) is the histograms of the input source data.

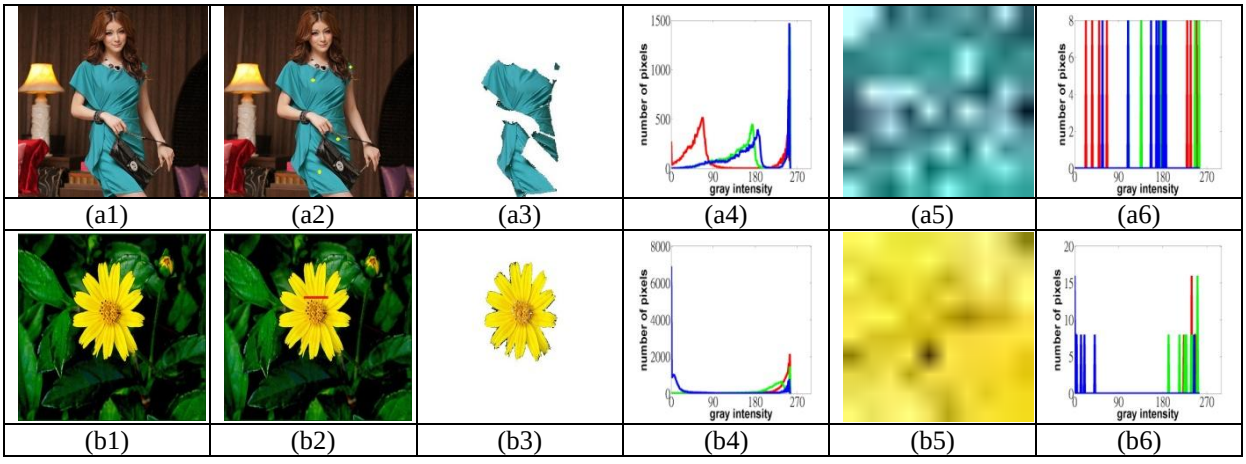

(a1) (a2) (a3) (a4) (a5) (a6)

(b1) (b2) (b3) (b4) (b5) (b6)

Fig. 2: The target object and source object.

The multiple regression analysis is used to find the best fitting functions (polynomials) of the three R, G, and B elements of these input data. These best fitting functions of MRA are used to find out the transferred R, G, and B values of each pixel of the target object. Fig. 3 shows the curves of the degree 1,

degree 5, and degree 9 best fitting functions of component R, G, and B between source object and target object. Table 1a, Table 1b, and Table 1c are respectively the tables of the best fitting functions' coefficients of component R, G, and B.

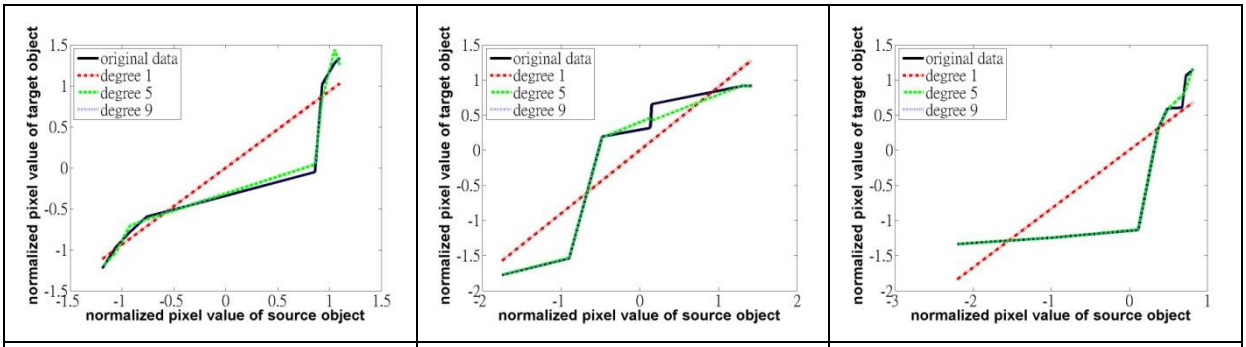

Fig.3: The curves of degree1, 5, and 9 best fitting functions on (a)R-plane, (b)G-plane, and (c)B-plane.

Table 1a: Coefficients of best fitting functions for R-component

	β9	β8	β7	β6	β5	β4	β3	β2	β1	β0
Degree 1	0	0	0	0	0	0	0	0	0.936108	-1.39E-17
Degree 2	0	0	0	0	0	0	0	0.371294	0.945084	-0.36549
Degree 3	0	0	0	0	0	0	1.230393	0.933688	-0.33362	-0.88982
Degree 4	0	0	0	0	0	-0.53087	1.208217	1.972992	-0.32718	-1.36455
Degree 5	0	0	0	0	-6.40635	-6.01339	13.95634	12.45405	-6.43331	-6.20865
Degree 6	0	0	0	-1.88509	-6.55713	-0.5606	14.14902	7.383578	-6.47023	-4.70037
Degree 7	0	0	25.3015	20.95617	-81.5416	-66.3267	86.96714	69.53883	-29.607	-23.975
Degree 8	0	11.97975	25.3015	-26.2141	-80.7814	1.767913	85.46556	26.89678	-28.8808	-14.2134
Degree 9	3.651561	8.23782	10.92347	-11.2485	-60.2628	-19.9594	72.93681	40.43754	-26.1322	-17.2625

Table 1b: Coefficients of best fitting functions for G-component

	β9	β8	β7	β6	β5	β4	β3	β2	β1	β0
Degree 1	0	0	0	0	0	0	0	0	0.898243	-2.84E-16
Degree 2	0	0	0	0	0	0	0	-0.24278	0.863474	0.238982
Degree 3	0	0	0	0	0	0	-0.28191	-0.36622	1.457789	0.320757
Degree 4	0	0	0	0	0	0.585044	0.266229	-1.70314	0.639458	0.463845
Degree 5	0	0	0	0	-0.76697	0.359387	2.640849	-1.68665	-0.57521	0.537954
Degree 6	0	0	0	6.504437	0.974573	-24.8832	-1.70067	20.16632	5.592219	-0.68138
Degree 7	0	0	321.7055	49.88963	-1259.86	-73.9716	1110.476	181.5941	-96.6869	7.42033
Degree 8	0	-77.6813	321.7055	355.7598	-1289.06	-344.15	1107.709	211.5707	-101.967	7.682886
Degree 9	11.85388	36.69704	275.0308	-90.1487	-1204.84	54.08443	1107.208	168.2388	-94.2324	7.296298

Table 1c: Coefficients of best fitting functions for B-component

	β9	β8	β7	β6	β5	β4	β3	β2	β1	β0
Degree 1	0	0	0	0	0	0	0	0	0.833448	6.94E-17
Degree 2	0	0	0	0	0	0	0	0.592896	1.607382	-0.58363
Degree 3	0	0	0	0	0	0	0.276821	1.143326	1.426145	-0.76976
Degree 4	0	0	0	0	0	-1.47532	-2.87513	2.519677	3.663813	-1.45445
Degree 5	0	0	0	0	4.811653	6.890788	-11.8146	-3.71294	9.036518	-2.09914
Degree 6	0	0	0	-8.42062	-5.06426	31.14399	-9.06945	-19.5895	14.99505	-2.58751
Degree 7	0	0	-359.544	-251.511	1244.234	-358.586	-753.139	566.0099	-127.454	7.197058
Degree 8	0	-634.089	-359.544	2245.213	-928.492	-1216.52	1165.657	-376.656	57.0983	-4.26028
Degree 9	199.7468	-655.81	-1146.05	3015.18	-732.659	-1850.36	1528.34	-467.084	67.02953	-4.65277

3. Experiment results

In this section, some experimental results under various conditions are shown to illustrate the utility and efficiency of the proposed scheme. The target RGB color image is a girl in a blue dress (496×372 pixels). The source color images with different sizes are blue roses (528×458 pixels), wool hat (450×377 pixels), potted plant (750×1000 pixels), amber (399×354 pixels) and carnation flower (640×480 pixels).

The RGB model cannot accurately and suitably describe human perception of color. Due to the high correlation of R, G, and B, a respective modification of the red, green and blue channels, may result an out-estimated color. Therefore, measures such as the color-difference and intensity-difference defined in the RGB color space are not appropriate to quantify the perceptual differences between images [11]. On the other hand, the numerical differences between colors in the CIELAB system is very consistent with human visual perceptions; the color distance in terms of CIELAB components really indicates how much the color transferred image differs from the source image. To present the color distance between the transferred image and source image with CIELAB component units is the most suitable way to measure the performance of color transferring schemes [12]. In order to give a detailed description of the color transfer results, several measurement metrics are conducted to measure the color transfer performance of the proposed algorithm. They are the difference in mean values of the color transferred image from the source image in lightness/ darkness (L^*), in red-shade/ green-shade (a^*), in yellow-shade/ blue-shade (b^*), in chromaticity (C^*), in hue (H^*), and in total color (E^*) [12, 13]. These performance measures are based on two images: a source color image and the color transferred image. These performance measures are described as follows:

$$C^* = \sqrt{(a^*)^2 + (b^*)^2}, \tag{7}$$

$$E^* = \sqrt{(L^*)^2 + (a^*)^2 + (b^*)^2}, \tag{8}$$

$$H^* = (180 \times \arctan 2(b^* / a^*)) / \pi, \tag{9}$$

$$\overline{X} = \sum_{j=1}^{N} X(j) / N, X \in \{L^*, a^*, b^*, C^*, H^*, E^*\}, \tag{10}$$

$$\Delta \overline{X} = \overline{X}_t - \overline{X}_s, \tag{11}$$

$$\Delta \overline{X}(\%) = 100 \times (|\Delta \overline{X}| / \overline{X}_s), \tag{12}$$

where $X(j), X \in \{L^*, a^*, b^*, C^*, H^*, E^*\}$ is the pixel value of pixel $p(j)$ in the X plane of original CIELAB color image; N is the size of the extracted object; $\overline{X}$ is the mean of X ; $\overline{X}_t$ is the mean of X component of color transferred target-object; $\overline{X}_s$ is the mean of X component of source object; $\Delta \overline{X}$ is the difference of X component mean of the transferred target-object from the source object; $\Delta \overline{X}(\%)$ is the difference ratio of X component mean of the transferred target-object from the source object; and arctan*2* is a more novel version (four quadrant) of the arc-tangent function that returns the angle in the full range ($-\pi$, π], and is defined as the following equation [14]:

$$\arctan 2\left(\frac{y}{x}\right) = \begin{cases} \arctan(y/x), x > 0 \\ \pi + \arctan(y/x), x < 0, y \geq 0 \\ -\pi + \arctan(y/x), x < 0, y < 0 \\ \pi/2, x = 0, y > 0 \\ -\pi/2, x = 0, y < 0 \\ \textit{undefined}, x = y = 0 \end{cases} \tag{13}$$

For testing images, these measurement metrics are evaluated by applying the proposed algorithm in the RGB domain. These measurement metrics are listed in tables for the performance analysis. Fig. 4 and Table 2 are used to demonstrate the color transferred results corresponding to the variation in the degree of best fitting polynomials (functions). Fig. 4 (T) is the original target object and Fig. 4 (S) is the source object. Fig. 4 (a*j*), *j*=1, 2, … , 8, represent the color transferred target-object obtains with the *j* best fitting function in the RGB color space. Fig. 5 shows the box-plots of L*, a*, and b* for the target object, source object, and color transferred objects on R, G,

and B planes, respectively. Column 1 indicates the R-component, Column 2 indicates the G-component, and Column 3 indicates the B-component. The following conclusions made are based on the above box plots. The higher degree multiple regressions are superior to the lower multiple regressions and the performances of the higher degree (larger than 2) best fitting functions are almost the same. The measurement metrics for the target, source and color transferred objects in Fig. 4 are arranged into Table 2. Table 2 shows the same conclusions as Fig. 4 and Fig. 5.

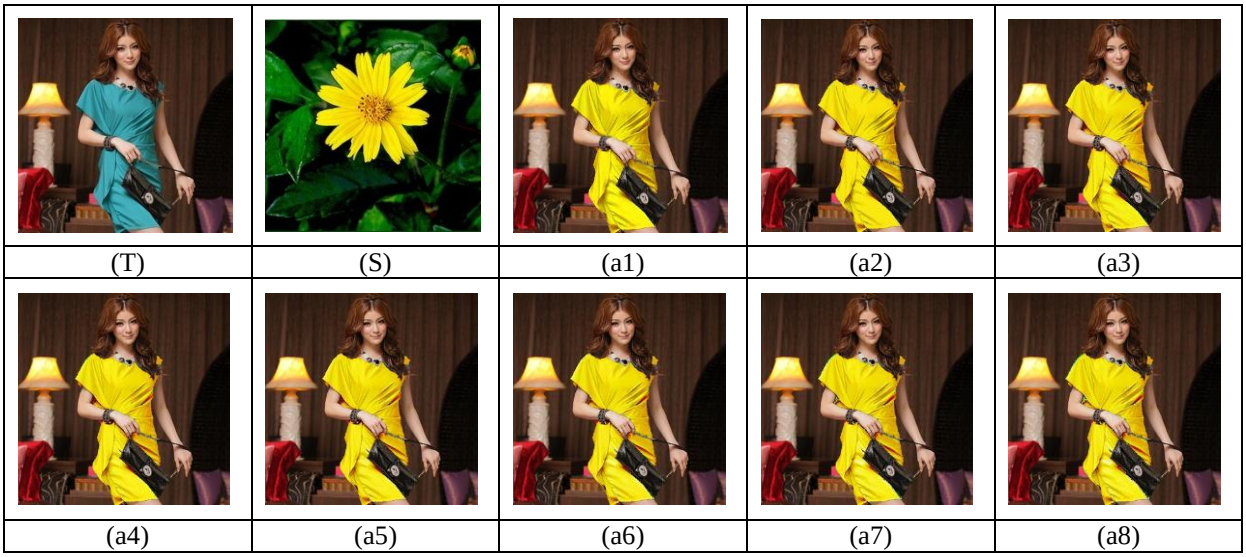

Fig. 4: The color transfer results corresponding to the variation in the degree of best fitting polynomials.

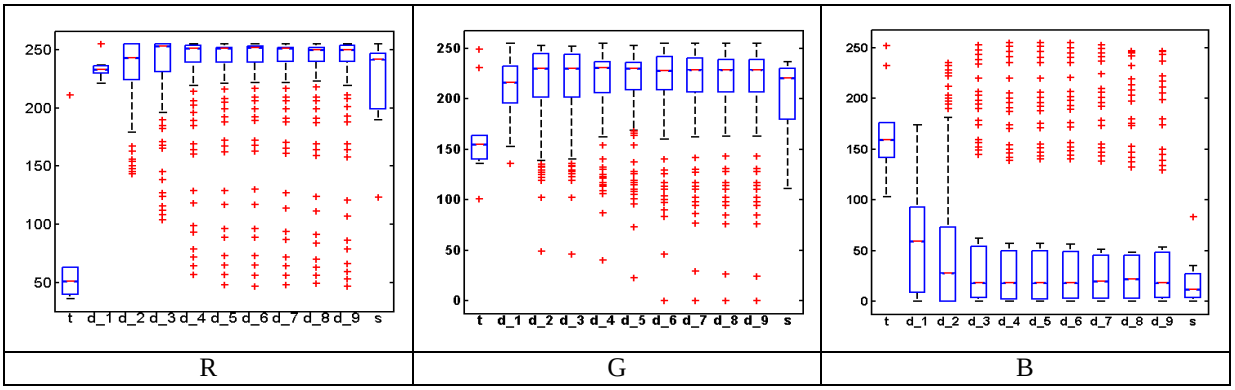

Fig. 5. The box-plots of L*, a*, and b* for the target, source, and color transferred objects in Figure. 4.

Table 2: The measurement metrics for the target, source and color transferred objects in Figure. 4

CIELAB	L*		a*		b*		C*		H*		E*	
	MEAN	STD	MEAN	STD	MEAN	STD	MEAN	STD	MEAN	STD	MEAN	STD
Dress	150.4304	51.46917	106.4236	8.978589	117.7709	5.477925	158.785	9.692401	42.04098	1.432582	221.7871	37.35482
chrysanthemum	215.6711	39.28094	124.7222	7.944162	200.1057	26.23079	236.5024	20.38787	32.30329	4.79458	321.9492	27.47353
Degree 1	217.8292	31.33225	123.6916	8.801648	195.9631	28.19823	232.6563	21.0893	32.71153	5.441701	320.2656	20.85404
Degree 2	220.7215	36.31317	125.5502	10.58648	196.3769	30.15897	234.1777	22.56435	33.08883	5.885266	323.7781	23.50912
Degree 3	220.227	35.17295	127.6649	10.90815	196.6029	29.94967	235.4517	23.01038	33.46908	5.704993	324.3933	21.74743
Degree 4	220.2034	33.89269	126.8906	11.99645	196.3171	30.07789	234.8753	22.88602	33.35077	5.926351	323.8914	20.56034
Degree 5	220.2727	33.9665	126.9508	11.82427	196.5536	29.75918	235.0651	22.79584	33.31984	5.809531	324.0879	20.39675
Degree 6	220.2781	33.79962	126.9951	11.82259	196.3766	30.00075	234.9625	22.8892	33.36195	5.875098	323.9999	20.49778
Degree 7	220.3988	33.6955	127.0985	11.97724	196.5681	29.82683	235.1607	22.92576	33.34757	5.816235	324.2254	20.37048
Degree 8	221.8867	30.26971	126.4629	11.09722	197.1577	29.23962	235.1959	22.91315	33.1205	5.521752	325.0135	18.92759
Degree 9	222.8437	29.33692	125.7097	11.85683	193.9913	29.53413	232.1507	23.54637	33.38938	5.610419	323.5097	17.60135

The source object extraction results and the recolor results with different source objects are illustrated in Fig.6 and the statistical values (mean, standard deviation (STD)) of the measurement metrics for each object in L*, a*, b*, C*, H* and E* are arranged into Table 3,Table 4 and Table 5. The items in Fig.6, row 1 shows the original source images, row 2 shows the marks (seeds) on the original source images, row 3 shows the source objects extracted by the proposed COEMT, row 4 shows the recolored objects by the proposed MRA, and row 5 shows the resultant images. The experiment results clearly show that the proposed algorithm provides superior results. Table 3, Table 4 and Table 5 demonstrate that these statistical values are almost the same between the source objects and the corresponding transferred objects obtained by using the proposed scheme.

Image	Blue roses	Wool hat	Potted plant	Amber	Carnation
Original source image					
	(a1)	(a2)	(a3)	(a4)	(a5)
Seeds	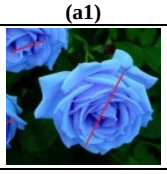	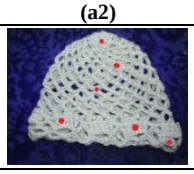	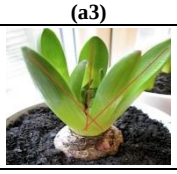		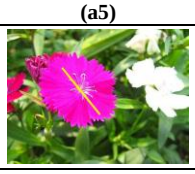
	(b1)	(b2)	(b3)	(b4)	(b5)
Extracted source object	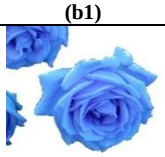	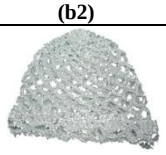	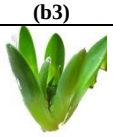		
	(c1)	(c2)	(c3)	(c4)	(c5)
Recolored object					
	(c1)	(c2)	(c3)	(c4)	(c5)
Result image					
	(d1)	(d2)	(d3)	(d4)	(d5)

Fig. 6: Examples of color transferring between objects with the proposed multiple regression analysis algorithm

Table 3: The measurement metrics for the target and source objects in Figure.6

CIELAB	L*		a*		b*		C*		H*		E*	
	MEAN	STD	MEAN	STD	MEAN	STD	MEAN	STD	MEAN	STD	MEAN	STD
Blue dress	150.4304	51.46917	106.4236	8.978589	117.7709	5.477925	158.785	9.692401	42.04098	1.432582	221.7871	37.35482
Blue roses	144.5743	41.92839	134.4017	13.13042	74.8278	16.13991	154.9887	8.626814	60.80493	6.876357	214.6325	26.2399
Wool hat	156.1177	40.65138	106.2356	13.22336	162.0112	22.88793	195.1399	12.36085	33.6504	7.001189	252.3068	24.4726
Potted plant	145.2159	37.93563	99.25579	9.785787	171.8834	14.54883	199.0365	9.355872	30.14659	4.365411	248.2776	24.25018
Amber	145.2163	36.49202	108.8427	21.26773	173.3229	14.33429	205.6276	16.20587	32.0184	5.473507	253.6519	25.00947
Carnation	147.3229	40.41436	150.0934	33.0741	80.18154	19.15783	171.5446	31.47177	61.45552	7.181401	229.2629	34.55282

Table 4: The measurement metrics for the color transferred target objects in Figure.6

CIELAB	L*		a*		b*		C*		H*		E*	
	MEAN	STD	MEAN	STD	MEAN	STD	MEAN	STD	MEAN	STD	MEAN	STD
Blue dress	163.3185	55.63949	128.5074	17.02557	90.41837	31.5838	160.0518	18.98476	55.31715	10.59851	231.9893	43.89292
Blue roses	188.8126	39.31711	126.2175	12.73377	130.3833	11.19284	181.8435	12.28983	44.02449	3.452397	264.1006	25.78697
Wool hat	162.4814	53.23631	102.4191	23.91867	162.4924	21.23415	194.4188	10.84952	32.27166	8.746327	257.2893	30.86813
Potted plant	168.2953	52.25107	142.5651	16.45696	164.566	21.28246	218.2576	22.22912	40.98129	4.046821	280.6464	20.53054
Amber	169.9814	47.76056	185.6286	33.01946	102.9685	16.23654	214.3661	21.48309	60.22578	8.366982	277.9231	18.64821
Carnation	163.3185	55.63949	128.5074	17.02557	90.41837	31.5838	160.0518	18.98476	55.31715	10.59851	231.9893	43.89292

Table 5: The absolute difference in measurement metrics of the transferred target-object from the source object in Figure. 6

CIELAB	ΔL*	ΔL*(%)	Δa*	Δa*(%)	Δb*	Δb*(%)	ΔC*	ΔC*(%)	ΔH*	ΔH*(%)	ΔE	ΔE*(%)
Blue roses	18.74422	11.47709	5.89427	4.586715	15.59057	17.2427	5.063121	3.163426	5.487778	9.920573	17.35684	7.481743
Wool hat	32.69487	17.31605	19.98188	15.83131	31.62791	24.25764	13.29639	7.311995	10.37409	23.56435	11.79375	4.46563
Potted plant	17.26554	10.62616	3.163266	3.088552	9.391059	5.779385	4.617675	2.375117	2.125071	6.584944	9.011727	3.502566
Amber	23.07898	13.71338	33.7224	23.65404	8.756862	5.321186	12.63007	5.786773	8.962891	21.87069	26.99445	9.618671
Carnation	22.6585	13.32999	35.5352	19.14317	22.78695	22.13002	42.82152	19.97588	1.229737	2.041878	48.66021	17.50852

4. Conclusions

Color is a significant feature of information for image classification, segmentation, recognition, analysis, and retrieval. It offers artists with the ability to show style and creativity, and also provides doctors a way to describe tissue pathology and aesthetics in dermatology and dentistry. Frequently, the colors in an object must be properly adjusted in advance due to some of the original colors in an object might not be suitable for analysis. Color transformation is one of popular techniques in image color processing for changing an image's color and preserving the image's original details and natural look at the same time. This paper presented a multiple regression analysis based algorithm for color transformation between objects. The experiment results show the proposed algorithm has three characteristics: (i) the proposed algorithm is simple, effective and accurate in transferring color between objects without any change in the object details, (ii) the proposed algorithm saves time and the time consumption is independent of the number of bins selected and the degree of regression, (iii) there are no restrictions in the dynamic ranges of colors of objects.

References

[1] Bosch , X. Mun˜oz, J. Freixenet, Segmentation and description of natural outdoor scenes, Image and Vision Computing, vol. 25, pp. 727–740, 2007.

[2] T. Pouli, E. Reinhard, Progressive histogram reshaping for creative color transfer and tone reproduction, Proceedings of the Symposium on Non-Photorealistic Animation and Rendering 2010, pp. 81- 90, 2010.

[3] S. De, A. Dagan, P. Roan, J. Rosen, M. Sinanan, M. Gupta, B. Hannaford, CIELab and sRGB color values of in vivo normal and grasped porcine liver, Proceedings of Medicine Meets Virtual Reality (MMVR 15) pp.109-111, 2007.

[4] S. Xu, S. Zhejiang, S. Zhang, and X. Ye, Uniform color transfer, Proceedings of IEEE International Conference on Image Processing, pp. 940-943, 2005.

[5] D. Freedman and P. Kisilev, Object-to-object color transfer: Optimal flows and SMSP transformations, 2010 IEEE Conference on Computer Vision and Pattern Recognition (CVPR), pp. 287 – 294, 2010.

[6] E. Reinhard, M. Ashikhmin, B. Gooch, and P. Shirley, Color transfer between images, IEEE Computer Graphics and Applications 21, pp. 34–41, 2001.

[7] D. L. Ruderman, T.W. Cronin, and C.C. Chiao, Statistics of cone responses to natural images: Implications for visual coding, J. Optical Soc. of America, vol. 15, no. 8, pp. 2036-2045, 1998.

[8] C. C. Liu, G. N. Hu, A re-coloring algorithm for a color image using statistic scheme in CIE L* a* b* color space, 2010 International Symposium on Computer, Communication, Control and Automation, pp. 240-243, May 5-7, 2010.

[9] C. Y. Huang, G. H. Tzeng, Multiple generation product life cycle predictions using a novel two-stage fuzzy piecewise regression analysis method, Technological Forecasting & Social Change, vol.75, no. 1, pp. 12- 31, 2008.

[10] C. C. Liu, G. N. Hu, A color objects extraction scheme using Dynamic thresholds, 2009 International Conference on Digital Content, Chungli, Taiwan, pp. 84-91, 2009.

[11] F. Lopez, J. M. Valiente, J. M. Prats, A. Ferrer, Performance evaluation of soft color texture descriptors for surface grading using experimental design and logistic regression, Pattern Recognition, vol. 41, pp. 1761 – 1772, 2008.

[12] M. E. Celebi, H.A. Kingravi, F. Celiker, Fast colour space transformations using minimax approximations, IET Image Process., vol. 4, no. 2, pp. 70–80, 2010.

[13] Y. Chen, P. Hao, Optimal transform in perceptually uniform color space and its application in image retrieval, 7th International Conference on Signal Processing (ICSP '04), vol. 2, pp. 1107- 1110, 2004.

[14] [14] P. Djeu, M. Quinlan, and P. Stone, Improving particle filter performance using SSE instructions, The 2009 IEEE/RSJ International Conference on Intelligent Robots and Systems, pp.3480- 3485, 2009.